Investigation on the Effect of an In-plane Auxiliary Field on the SNR of HAMR Recording Systems

Hongtao Wang, Chan Kheong Sann, Zhimin Yuan, and Sophoclis Alexopoulos Pantelis

Data Storage Institute, Agency for Science, Technology, and Research (A*STAR), Singapore 117608

In this work, we consider the application of an in-plane auxiliary field into the Exchange-Coupled Composite (ECC) medium in the Heat-Assisted Magnetic Recording (HAMR) system. The dynamic micromagnetic simulations are conducted based on the Landau-Lifshitz-Bloch (LLB) equations and the SNR characterizations are performed. The effect on the Signal-to-Noise Ratio (SNR) of the HAMR system is investigated. The improvement on the SNR with the auxiliary field in negative down-track direction is identified.

***Index Terms*—Heat-assisted magnetic recording, Magnetic heads, Micromagnetic simulation, Signal Processing, Near field optical transducer.**

I. Introduction

Heat Assisted Magnetic Recording (HAMR) is one of the promising approaches to achieve ultrahigh density storage in Hard Disk Drives (HDDs) [1]. Recording in HAMR systems is realized when the grains are flipped to the desired orientation by introducing heat from a laser to assist the magnetic field. This allows for the medium grains to be reduced in size while maintaining the thermal stability ratio by making the anisotropy of the grains large. Meanwhile, the recording density in the HAMR system is limited by many factors such as the material properties, the Curie temperature, thermal spot size, writing field distribution and so on. Possible recording density for HAMR is studied via whole system simulations [2][3]. To increase the recording density of HAMR systems, the effects of the media structure and its material properties on the cross track thermal spot size and down-track thermal gradient of recording layer are also discussed [4][5]. To improve the recording performance for given thermal profiles, we introduce an in-plane auxiliary field into an exchange coupled composite (ECC) media in the HAMR system to help the changing of the gradient down-track recording field. In this study, the micromagnetic model is built via the Landau-Lifshitz Bloch (LLB) equations [6][7] to simulate the grains during HAMR recording. The magnetization distributions are obtained from the micromagnetic simulations for the HAMR system. The Signal-to-Noise Ratio (SNR) after convolution of the granular medium profile with a read head sensitivity (RHS) function [8] is utilized to measure the recording performance. In this work, we study and identify the influence of an in-pane auxiliary field on the SNR performance of the HAMR system with ECC media. In these micromagnetic simulations, the in-pane auxiliary field is assumed to be in the both of negative and positive down-track directions. The media of the micromagnetic model in this study has two exchange coupled layers. To investigate the effects of the auxiliary field, the sigma of easy-axis angle σ_{ez} and the interlayer exchange coupling coefficient H_{ex}/H_k are treated as variables in our simulations.

Manuscript received March 7, 2014.

Corresponding author: Hongtao Wang (e-mail: wang_hongtao@dsi.a-star.edu.sg).

Color versions of one or more of the figures in this paper are available online at http://ieeexplore.ieee.org.

Digital Object Identifier inserted by IEEE

II. The Model And Processing

A. Write Head, Thermal Spot and Media

An unshielded single pole write head [9] is used in this study. The magnetic write field was calculated by the Finite Element Model (FEM). The main pole is 60 nm width and 100 nm thickness at the air bearing surface (ABS). One edge of the main pole is with 90° angle and the heat source is placed 22.5 nm away from the edge. The distributions of write field for the top and bottom layers of the media are shown as Fig. 1.

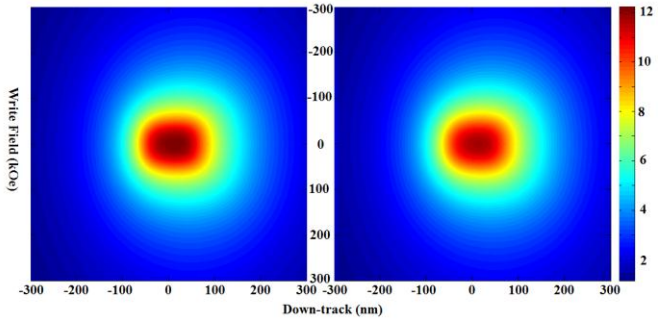

Fig. 1. Write field distribution (left: top layer; right: bottom layer).

The heat source originates from a near field optical transducer (NFT) with a lollipop shape and made of gold (Au) with disk diameter of 150 nm and tip length of 10 nm. Fig. 2 shows the model of the relevant parts of the write head and the NFT and their locations. The thermal conductivity of FePt is assumed to 5 W/m/K (in-plane) [4][5]. The boundary thermal resistance (BTR) between adjacent layers is assumed to be 2×10^{-9} m^2K/W. The environment temperature, the heated peak temperature in the top layer and in the bottom layer of the media are assumed to be 300K, 800K and 612K respectively. The distributions of thermal spots obtained from simulation of the NFT for the top and bottom layers are shown as Fig. 3.

The medium is modelled as a dual-layer Voronoi diagram. The grain size is set to 5 nm and the grain pitch is 5.5 nm with 18% distribution. The thicknesses of both the top and bottom layers are 5nm. The spacing between the top layer and the

bottom layer is 1 nm. The saturation magnetisations of the top and bottom layers are both 800 emu/cc with sigma of 3%. The anisotropy fields (H_k) of both layers are of 60 kOe and also with sigma of 3%. The inter-granular exchange coupling constant (A_x) of both layers are 1×10^5erg/cm^3 with sigma of 3%. The Curie temperatures are 780K for the top layer and 600K for the bottom layer, both with sigma of 3%. The sigma of the easy-axis angle is assumed as a variable from 0° to 5°.

B. Micromagnetic Modeling and SNR Characterization

The micromagnetic simulations are used to model the recording physics of the dual layer exchange coupled HAMR. The dynamics of the Voronoi grains in the layers are modelled using the form II of Landau-Lifshitz-Bloch (LLB) equation, which has been improved and proposed as a more consistent model of the microspin dynamics at elevated temperatures [7]. Therefore, the behaviour of the grains around and above the Curie temperature T_c can more accurately be modelled. The form II of the LLB formulation is given by equation (1),

$$\frac{\partial \vec{m}}{\partial t} = -\gamma\left[\vec{m}\times\vec{H}\right] + \frac{|\gamma|\alpha_{\parallel}}{m^2}\left[\vec{m}\cdot\vec{H}\right]\vec{m} - \frac{|r|\alpha_{\perp}}{m^2}\left[\vec{m}\times\left[\vec{m}\times\left(\vec{H}+\eta_{\perp}\right)\right]\right] + \eta_{\parallel}. \quad (1)$$

where $\vec{m}$ is the magnetization vector of a grain, $\vec{\mathbf{H}}$ is the effective field, γ is the gyromagnetic constant, $\alpha_{\parallel}$ and $\alpha_{\perp}$ are dimensionless longitudinal and transverse damping parameters given in equations (2) and (3). In those equations T and T_c are the temperature and the Curie temperature and λ is the parameter describing the coupling of the spins to the heat bath on an atomistic level. And when T is above T_c, $\alpha_{\parallel}$ and $\alpha_{\perp}$ are equal and given by equation (3),

$$\alpha_{\parallel} = \lambda\frac{2T}{3T_c} \quad \alpha_{\perp} = \lambda\left[1-\frac{T}{3T_c}\right] \quad T < T_c \quad (2)$$

$$\alpha_{\parallel} = \alpha_{\perp} = \lambda\frac{2T}{3T_c} \quad T \geq T_c \quad (3)$$

In (1), the statistical properties of the fluctuating terms $\eta_{\parallel}$ and $\eta_{\perp}$ are given by equation (4) in terms of the fluctuation-dissipation theorem and the Fokker-Planck equation [10],

$$\begin{aligned} \left\langle \eta_i^{\mu} \right\rangle &= 0, \\ \left\langle \eta_i^{\perp}(0)\eta_j^{\perp}(t)\right\rangle &= \frac{2k_B T(\alpha_{\perp}-\alpha_{\parallel})}{|\gamma|M_s^0 V\alpha_{\perp}^2}\delta_{ij}\delta(t), \\ \left\langle \eta_i^{\parallel}(0)\eta_j^{\parallel}(t)\right\rangle &= \frac{2|\gamma|k_B T\alpha_{\parallel}}{M_s^0 V}\delta_{ij}\delta(t), \\ \left\langle \eta_i^{\parallel}\eta_j^{\perp}\right\rangle &= 0. \end{aligned} \quad (4)$$

where $\mu = \parallel$ and $\perp$, indices i, j denote components x, y, and z, k_B is the Boltzmann constant, M_s^0 is the saturation magnetization of the grain at the temperature of 0 K, and V is the volume of the grain.

The SNRs computed in this study are obtained from a signal-processing perspective. The signal is taken as the noise-free output y_k of the best fit linear response h to the input bits a_k, while the noise is taken as the difference between the noise-free signal and noisy observed signal r_k. The best fit linear response h is obtained by solving the Wiener-Hopf [11] equation that uses the autocorrelation matrix of a_k and the cross-correlation matrix between a_k and r_k. In the context of Figure 4, the SNR is then obtained as the ratio of the powers:

$$SNR = 10*\log_{10}\left[\frac{E\left(y_k^2\right)}{E\left(e_k^2\right)}\right] \quad (5)$$

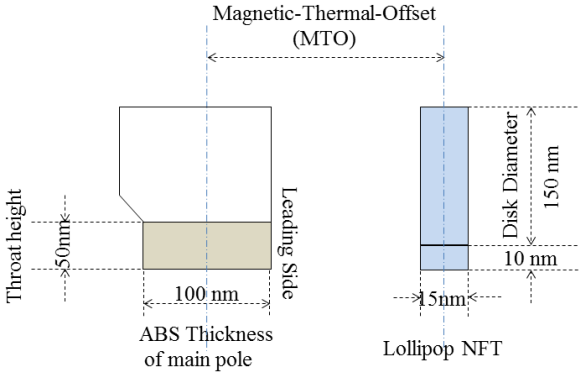

Fig. 2. The model of the relevant parts of the write head and the NFT and their locations.

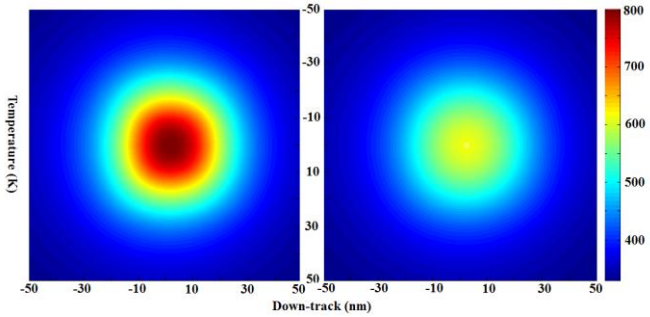

Fig. 3. Thermal spot distribution (left: top layer; right: bottom layer).

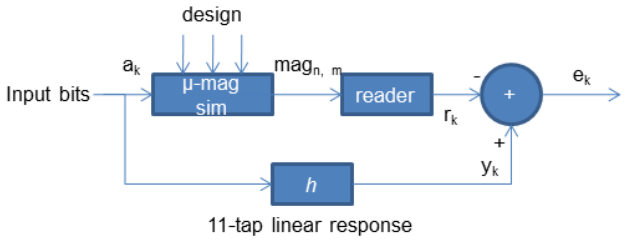

Fig. 4. Block Diagram showing components used in the SNR calculation.

III. Experiments, Results And Discussion

A. Experiments

In this study, the auxiliary field is chosen from nine values from 0 Oe to -800 Oe respectively. Note, the negative sign means the auxiliary field is in the negative down-track direction. σ_{ez}, the sigma of the easy-axis angle is treated as a variable and set to six values between 0° and 5° while the mean of the easy-axis angle is 90° to the surface of the medium. In addition, we also vary the interlayer exchange field in the range H_{ex}/H_k = [0.1, 0.2, 0.3, 0.4, 0.5]. This depicts the various situations from weak to strong interlayer exchange coupling between the grains in the top and bottom layers. Given the parameter ranges on the auxiliary field, the easy axis distribution and interlayer exchange coupling mentioned above, there are 270 micromagnetic simulations in total, of 500 bits each carried out in this stage.

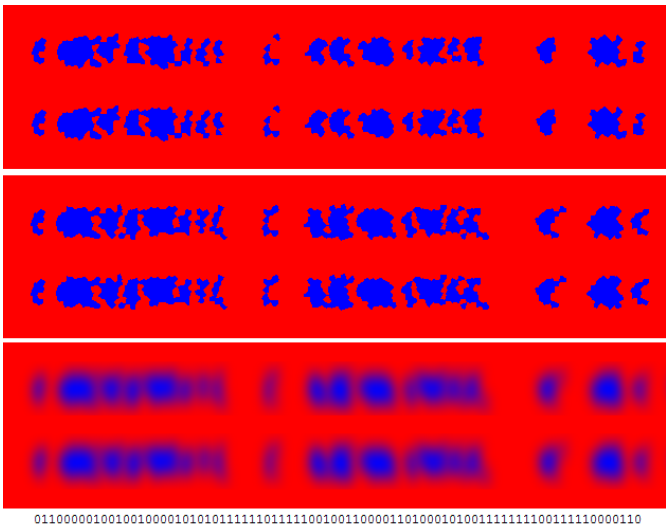

Fig. 5. A partial view of the magnetization profile of the HAMR recording with bit pattern and 2D read-back signal after convolution: H_{ex}/H_k = 0.3, σ_{ez} = 3° (Top: H_{aux} = 0 Oe; Middle: H_{aux} = -600 Oe; Bottom: read-back signal after convolution with the RHS functions while H_{aux} = -600 Oe;).

Fig. 5 shows a set of partial views of magnetization profiles obtained from the micromagnetic simulations for both of the top and bottom layers, in which H_{ex}/H_k = 0.3, σ_{ez} = 3°, and the auxiliary field H_{aux} = [0 Oe, -600 Oe] and one set of read-back signal after convolution with the RHS functions while auxiliary field equals to -600 Oe.

The magnetization distributions in both the top and bottom layers are shown in Fig. 5 for each of the listed auxiliary field s. From these two profiles, we can qualitatively see that the auxiliary field is having an effect on the writing of the top and bottom layers. To characterize the SNR from the results of micromagnetic simulations, read head sensitivity (RHS) functions based on a magnetic tunnel junction reader design [8] are used. The read-back signal is generated by the convolution of the RHS functions with the magnetization distributions from the micromagnetic simulations.

B. *Results and Discussion*

Fig. 6 shows the SNRs obtained from the micromagnetic simulations with the setting of H_{ex}/H_k of 0.1 and 0.5. For every simulation with the setting of H_{ex}/H_k, the auxiliary field is chosen from nine negative values between 0 Oe to -800 Oe and σ_{ez} is varied from 0° to 5°. With the increasing of the amplitude of the auxiliary field, the SNR goes up at first, then reaches to the highest value, and goes down at last. When H_{ex}/H_k = [0.1, 0.2, 0.3, 0.4, 0.5] respectively, the maximum SNRs are increased by about 3.5 dB from original setting.

TABLE I
THE ORIGINAL SNR, THE MAXIMUM SNR AND THE CORRESPONDING AUXILIARY FIELD WHEN σ_{ez} = 3°

H_{ex}/H_k	Original SNR	Maximum SNR	Corresponding Auxiliary Field
0.1	8.87 dB	12.24 dB	-300 Oe
0.2	8.89 dB	12.51 dB	-400 Oe
0.3	9.53 dB	13.10 dB	-400 Oe
0.4	8.87 dB	12.37 dB	-500 Oe
0.5	8.80 dB	12.34 dB	-600 Oe

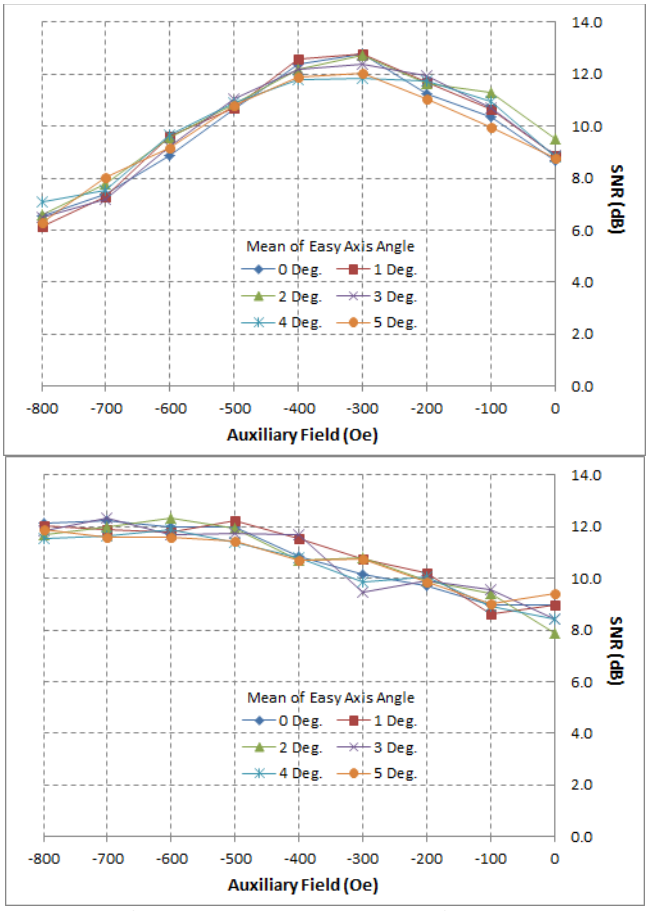

Fig. 6. SNR of the HAMR recording with H_{aux} of 0 Oe to -800 Oe when H_{ex}/H_k = 0.1 (top), 0.5 (bottom) respectively.

Table I lists the original SNR (without the auxiliary field), the maximum SNR and the corresponding auxiliary field, at which the maximum SNR is obtained, with σ_{ez} = 3° and different values of H_{ex}/H_k. From this table, we find that the SNRs are increased by an average of about 3.5 dB with the corresponding auxiliary field. Separately, the amplitudes of the increasing SNR are insignificant for different settings of H_{ex}/H_k. However, the corresponding auxiliary field, at which the maximum SNR is obtained, is different as the H_{ex}/H_k is changed. It is found that the higher auxiliary field is needed for larger values of H_{ex}/H_k.

Fig. 7 plots how the SNR changes in correspondence with

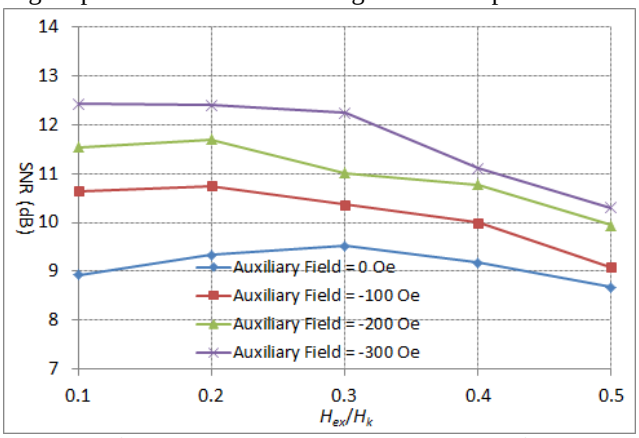

Fig. 7. SNR of the HAMR recording while the H_{ex}/H_k is set from 0.1 to 0.5 and σ_{ez} = 3°.

H_{ex}/H_k when the different auxiliary field is applied. The highest SNR is obtained with H_{ex}/H_k = 0.3 when there is no auxiliary field applied. As the amplitude of the auxiliary field is increased to 100 Oe and 200 Oe, the highest SNR is obtained with the H_{ex}/H_k = 0.2. Once the amplitude of the auxiliary field is increased to 300 Oe and more, the highest SNR is obtained when the H_{ex}/H_k = 0.1.

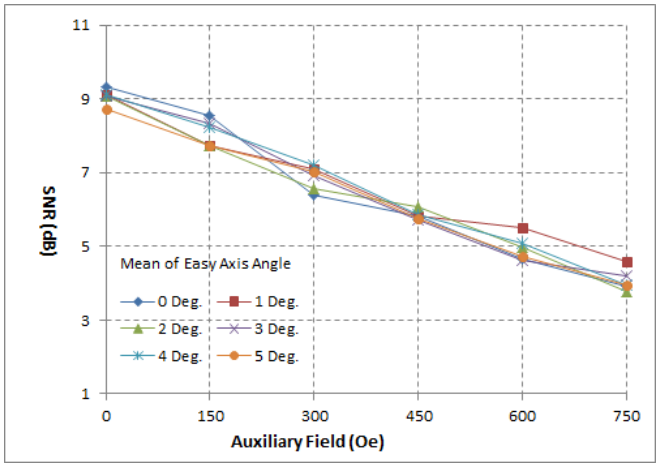

Fig.8. SNR of the HAMR recording while an auxiliary field in the down-track direction is applied (H_{ex}/H_k = 0.1).

C. *Further Simulations and Discussion*

In order to verify the results obtained from the above analysis, we also conduct a set of micromagnetic simulations in which the auxiliary field is in the down-track direction. In this set of simulations, the auxiliary field is chosen from six positive values between 0 Oe to 750 Oe, the H_{ex}/H_k is also set from 0.1 to 0.5, and σ_{ez} is the same as previously. Fig. 8 shows the effects of the positive direction auxiliary field on the SNR of the HAMR system when H_{ex}/H_k = 0.1 and $\sigma_{ez} = 3^o$. The results show that the higher down-track direction auxiliary field makes the recording performance worse.

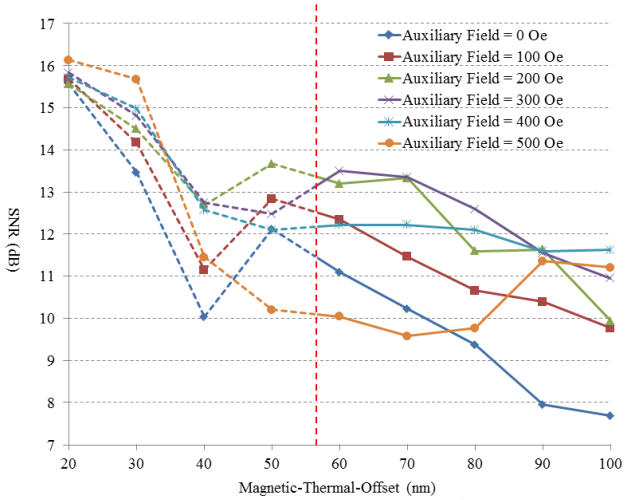

Fig.9. SNR of the HAMR recording while an auxiliary field in the down-track direction is applied (H_{ex}/H_k = 0.1).

Fig. 9 shows the SNRs when H_{ex}/H_k = 0.1 and $\sigma_{ez} = 3^o$ while the Magnetic-Thermal-Offset (MTO) is being changed. It can be found that different auxiliary field is required to reach the best SNR when the MTO is different. It should be noted that the part of dot-line is impractical in this figure as the minimum value of the MTO is 57.5 nm.

IV. Conclusion

In this work, we study the influence when an in-plane auxiliary field is included in a dual-layer HAMR ECC media. The very important point is the direction of the auxiliary field. The improvement of the recording performance is significant when an auxiliary field in the negative down-track direction is applied. A HAMR system with the best SNR value can be obtained with an appropriate auxiliary field for a given H_{ex}/H_k and sigma of easy-axis angle. Additionally, to reach the best SNR, the higher amplitude of the auxiliary field is required when the interlayer exchange coupling coefficient H_{ex}/H_k is higher. Practically, the auxiliary field can be obtained from a couple of sources. One possibility is including a longitudinal hard-magnet in the head that produces such a field, in a similar orientation to how longitudinal heads produce in-plane fields. A second possibility is that an additional magnetic layer in the medium with high K_u and in-plane magnetization could provide the needed in-plane auxiliary field.

Acknowledgment

The authors would like to thank Dr. Baoxi Xu from Data Storage Institute, A*STAR, Singapore for his contribution on the thermal profiles, and Dr. Yasushi Kanai from Niigata Institute of Technology, Japan for his contribution on the write field profiles.

References

[1] M. H. Kryder, E. C. Gage, T. W. McDaniel, W. A. Challener, R. E. Rottmayer, G. P. Ju, Y. T. Hsia, M. F. Erden, “Heat Assisted Magnetic Recording”, *Proceedings of the IEEE*, vol. 96, no.11, pp. 1810-1835, 2008.

[2] X. B. Wang, K. Z. Gao, H. Zhou, A. Itagi, M. Seigler, and E. Gage, “HAMR recording limitations and extendibility”, *IEEE Trans. Magn.*, vol. 49, pp. 686-692, 2013.

[3] S. J. Greaves, Y. Kanai, and H. Muraoka, “Thermally assisted magnetic recording at 4 Tb/in^2”, *IEEE Trans. Magn.*, vol. 49, pp. 2665-2670, 2013.

[4] B.X. Xu, Z.J. Liu, R. Ji, Y.T. Toh, J.F. Hu, J.M. Li, J. Zhang, K.D. Ye, and C.W. Chia, ‘Thermal issues and their effects on heat-assisted magnetic recording system”, *J. Appl. Phys.*, vol. 111, p. 07B701, 2012.

[5] B. X. Xu, Z. H. Cen, J. H. Goh , J. M. Li , K. D. Ye, J. Zhang , H. Z. Yang, Y.T. Toh, and C.G. Quan, “HAMR Media Design in Optical and Thermal Aspects”, *IEEE Trans. Magn.*, vol. 49, pp. 2559-2564, 2013.

[6] R. F. L. Evans, D. Hinzke, U. Atxitia, U. Nowak, R. W. Chantrell, and O. Chubykalo-Fesenko, “Stochastic form of the Landau-Lifshitz-Bloch equation”, *Physics Review B* 85, 014433 (2012).

[7] N. Kazantseva, D. Hinzke, U. Nowak, R. W. Chantrell, U. Atxitia, and O. Chubykalo-Fesenko, “Towards multiscale modeling of magnetic materials: Simulations of FePt,” *Phys. Rev. B* 77, 184428 (2008).

[8] Z. M. Yuan, C. L. Ong, S. H. Leong, T. Zhou, and B. Liu, “3-D sensitivity function of shielded reader by reciprocity principle,” *IEEE Trans. Magn.*, vol. 46, no. 6, pp. 1929–1932, Jun. 2010.

[9] S. J. Greaves, Y. Kanai, and H. Muraoka, “Magnetization Switching in Energy Assisted Recording”, *IEEE Trans. Magn.*, vol. 48, no. 5, pp. 1794-1800, May 2012.

[10] C. W. Gardiner, *Handbook of stochastic methods for Physics, Chemistry and the natural sciences*, (Springer, Berlin-New York, 2004).

[11] Sebastian Seung, “Wiener-Hopf equations. Convolution and correlation in continuous time”, http://hebb.mit.edu/courses/9.29/2004/lectures/lecture03.pdf.